www.czasopisma.pan.pl PAN POLSKA AKADEMIA NAUK www.journals.pan.pl

Arch. Min. Sci. **71** (2026), 1, 143-159

Electronic version (in color) of this paper is available: http://mining.archives.pl

DOI: https://doi.org/10.24425/ams.2026.157760

BARBARA DUTKA[1*], KATARZYNA SUŁKOWSKA[1]

STUDIES ON THE PORE STRUCTURE AND CO_2 ADSORPTION PERFORMANCE OF DIFFERENT RANK COALS

The study focuses on the analysis of pore structure and the determination of CO_2 adsorption properties of different rank coals originating from the Upper Silesian Coal Basin. Measurements were performed using a low-pressure volumetric apparatus ASAP 2020, Micromeritics, for sample porosity characterisation, and a gravimetric analyser IGA-001, Hiden Isochema, for gas adsorption measurements in the range of elevated adsorbate pressures. CO_2 adsorption isotherms were determined in the CO_2 pressure and temperature, 0-100 kPa at 0°C and 0-1200 kPa at 30°C, respectively. Coal investigations were complemented by microscopic, technical and densimetric analyses. CO_2 adsorption studies showed the absence of a universal model that adequately describes both low-pressure and elevated-pressure processes. Adoption of the Langmuir-Freundlich model proved appropriate for most coals (5 of 6), while for one sample (CR2), a better fit was obtained with the Freundlich model. The analyses confirmed differences in the pore structure and CO_2 adsorption properties of coals with different rank. With increasing degree of coalification, an increase in specific surface area and micropore volume was observed. All coals exhibited narrow micropores with sizes <0.7 nm (ultramicropores). Analysis of pore size distributions by the DFT method showed that the porous structure of the coals was crucial for assessing CO_2 adsorption performance and the transport properties of coal. The diffusion rate was not limited by the high rank of coal but rather by the structural heterogeneity of the pores, which could be detected by analysing the pore size distribution.

Keywords: Coal; CO_2; adsorption; pore structure; textural properties; effective diffusion coefficient; coal rank

1. Introduction

Carbon dioxide (CO_2) is a gas responsible for the greenhouse effect. The primary cause of the increase in CO_2 concentration in the atmosphere is the combustion of fossil fuels for energy

[1] STRATA MECHANICS RESEARCH INSTITUTE OF THE POLISH ACADEMY OF SCIENCES, 27 REYMONTA STR., 20-059 KRAKÓW, POLAND

* Corresponding author: dutka@imgpan.pl

production and extensive development of the industrial sector. In the context of ongoing climate change and the need to reduce greenhouse gas emissions, research on carbon dioxide capture and its economic utilisation is gaining increasing importance [1]. One of the significant directions of this research is the application of coal – a material with a well-developed porous structure and diverse surface properties – both as a sorbent and as a geological CO_2 storage medium [2,3]. Hard coal can be treated as a gas adsorbent that attracts and retains CO_2 molecules on the internal surface through the process of adsorption. Deep and so far unexploited coal seams have for years been perceived as promising geological structures for carbon dioxide storage [1]. A key challenge remains the issue of reducing coal permeability, which occurs as a result of the swelling of the coal matrix during CO_2 adsorption at high pressures. This effect limits the possibility of CO_2 injection and results in insufficient utilisation of the sorption capacity of the deposit [4-6]. In recent years, the number of carbon capture and storage (CCS) projects in coal seams and other geological formations has increased, both in the operational phase and in planned stages [7,8]. The increase in CCS projects creates new economic opportunities and supports the energy transition. Although at current CO_2 emission allowance prices, the use of CCS technologies remains economically unviable, such projects are also being planned and prepared in Poland. In general, mining areas and regions with a high concentration of coal deposits, particularly in Europe, are usually located near large sources of carbon dioxide emissions, while at the same time being significantly distant from its storage sites [9]. The ongoing reduction in coal extraction makes shallower deposits increasingly accessible for low-CO_2 emission projects [10].

Deep coal seams usually retain their original character and contain significant amounts of methane [1]. Injecting carbon dioxide into coal seams where methane naturally occurs increases the efficiency of coalbed methane (CBM) recovery, which is an environmentally friendly energy source. CO_2 injected into coal seams displaces methane through the mechanism of exchange adsorption and is preferentially adsorbed in the pore structure of coal [11]. The ability of coal to adsorb carbon dioxide depends on a number of factors, among which the degree of coalification plays a key role, influencing the development of microporosity, the nature of functional groups, and the physicochemical interactions with CO_2 [12-16]. As the degree of coalification increases, the aromaticity of the organic matter increases, accompanied by a decrease in the oxygen and hydrogen content. Coals with a higher degree of coalification generally exhibit a stronger affinity for CO_2 and a higher heat of adsorption, which results from the dominance of micropores with high surface energy. In contrast, coals with a lower degree of coalification, containing a greater number of oxygen-containing groups and mesopores, are characterised by lower energy density but greater swelling capacity and higher chemical reactivity [17-19].

The determination of pore structure and interpretation of textural parameters are key elements in characterising the adsorption potential of coals [12,20,21]. Numerous studies confirm that micropores (<2 nm) constitute the main binding sites for CO_2 molecules, while mesopores and macropores serve as diffusion channels and transport reservoirs [20,22]. The microporous space of coal contains a significant proportion of voids up to 0.7 nm in size (ultramicropores), where adsorption occurs through the mechanism of volume filling [23].

An important element in assessing the adsorption properties of coals is the influence of measurement conditions such as pressure, temperature, humidity, or sample preparation state (drying, grinding) – as each of these factors can significantly modify the obtained adsorption parameters [24]. Under real conditions, typical for industrial or geological applications, additional aspects must be considered, such as swelling of the coal matrix and the potential decrease in

adsorption capacity as a result of repeated saturation and desorption cycles [25,26]. Increased pressure promotes higher CO_2 adsorption capacity, while elevated temperature leads to its reduction, due to the exothermic nature of the phenomenon [11,20]. The rate of CO_2 adsorption in coal is governed by diffusion within the coal pores. Due to the complex pore structure of hard coals, encompassing pores of various sizes, the overall diffusion process includes several mechanisms. The parameter defining the rate of CO_2 diffusion in the porous structure of coal is the effective diffusion coefficient. This process can be considered in the context of both CO_2 accumulation in coal and the symmetric phenomenon of its release. The ability of coal to adsorb CO_2 results from the multifaceted interaction between porous microstructure, degree of coalification, and process conditions. Understanding these relationships is fundamental both for the optimal design of materials with high adsorption capacity and for the reliable assessment of the potential for geological CO_2 storage in coal deposits or enhanced coalbed methane recovery.

The study investigates the influence of the degree of coalification and pore structure of coals with different ranks on the adsorption capacity for CO_2 and the effective diffusion coefficient of CO_2 in coal. Based on adsorption measurements – both low-pressure and gravimetric under elevated CO_2 pressures – the fit quality of well-known gas adsorption models on hard coal was analysed. Particular attention was paid to the impact of the adopted isotherm model on the quality of approximation of experimental points in different pressure ranges of the adsorbate.

2. Materials and methods

2.1. Coals

The study was conducted on six hard coal samples with varying degrees of coalification. The coals originated from the Upper Silesian Coal Basin, a Polish-Czech geological region with the largest hard coal reserves in both countries. Most of the coal material was obtained from the Czech part of the USCB, known as the Ostrava-Karviná Basin, while two samples were collected from the Polish part, from the Jastrzębie-Zdrój area of the basin. Fig. 1 presents the location of the Upper Silesian Coal Basin and a lithostratigraphic profile illustrating its geological structure along with marked formations from which the coal samples were taken. According to the shown profile, younger layers overlie older ones in terms of geological age, which determines the degree of coalification of individual coal seams.

2.2. Sample characterisation methods

Coal samples were characterised to determine the properties resulting from the varying degree of coalification of coal. The characterisation was carried out based on the technical and microscopic examination. Each sample was crushed and divided into appropriate grain fractions, in accordance with the requirements of the individual analyses. The technical analysis included the determination of volatile matter, ash and total moisture contents of different rank coals, in accordance with standards PN-ISO 562:2000, PN-ISO 1171:2002, and PN-ISO 18134-1:2022. Density was determined from helium pycnometry using AccuPyc 1340 (Micromeritics). To determine the mean vitrinite reflectance (R_0), an Olympus BX50 polarisation microscope was used at 400× magnification. Polished sections were analysed in monochromatic light with oil immer-

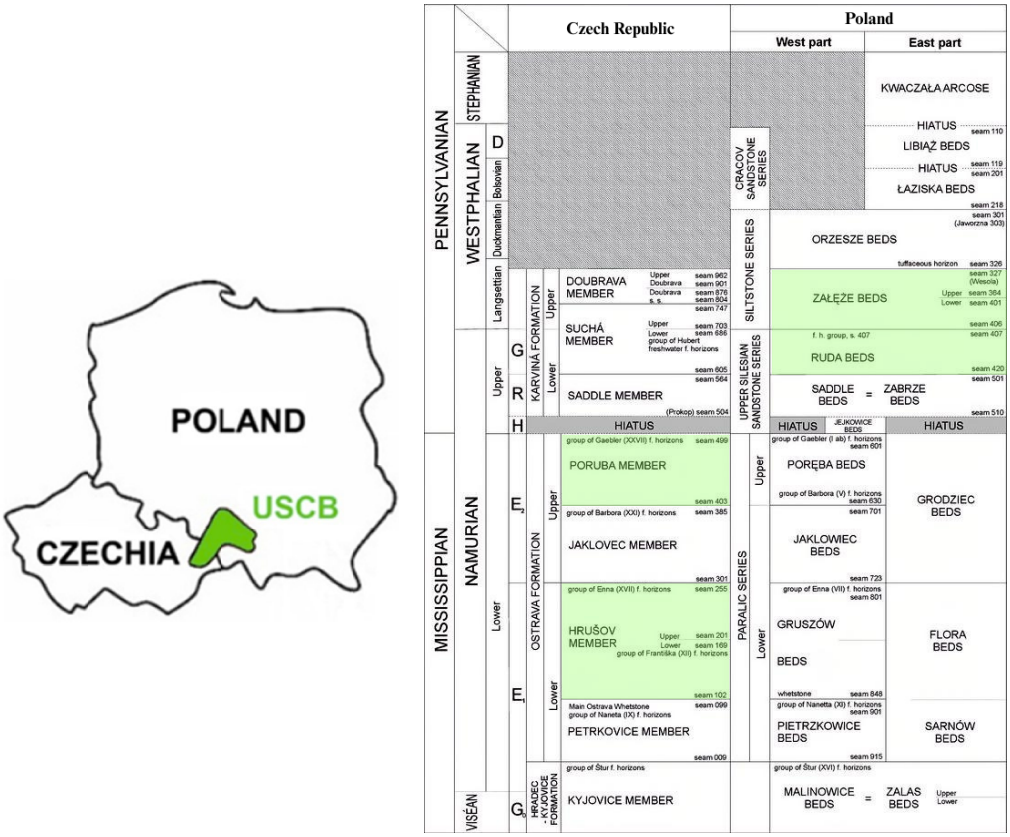

Fig. 1. Location of the Upper Silesian Coal Basin (USCB) and lithostratigraphic profile with marked layers from which the coals used in the study were collected (modified after Sivek et al. 2003 [27])

sion according to ISO 7404-5:2009. Results were obtained using the "LUCIA Vitrinite" image analysis system [28]. Based on vitrinite reflectance, the coal rank of the samples was determined. For petrographic analyses, a ZEISS AxioPlan polarisation microscope was used. The composition of the main maceral groups – vitrinite, inertinite, and liptinite – was determined based on 1500 measurement points in reflected white light, using oil immersion and 500× magnification according to ISO 7404-3:2009.

2.3. CO_2 adsorption studies

2.3.1. Low-pressure adsorption method

Low-pressure CO_2 adsorption measurements were carried out at a temperature of 0°C within the equilibrium pressures p from 0 to 100 kPa and relative pressures p/p_0 from approximately 10^{-6} to 0.029, where p_0 represented the saturation vapour pressure of CO_2 at the measurement temperature. The aim of CO_2 adsorption was to characterize the texture of the studied coal samples.

CO_2 adsorption isotherms were measured using a volumetric analyser ASAP 2020 (Micromeritics Instrument Corporation, United States). Coal samples with a grain fraction of 0.16-0.25 mm were degassed at 80°C under high vacuum conditions (~10^{-6} kPa) for 1440 minutes. The amount of the adsorbed CO_2 was approximated using the theoretical Langmuir isotherm:

$$a(p) = \frac{a_m bp}{1 + bp} \tag{1}$$

and the empirical Freundlich model:

$$q(p) = kp^n \tag{2}$$

where: a is the adsorbed amount of CO_2, cm^3/g STP, p is the equilibrium CO_2 pressure, kPa, a_m, cm^3/g STP – Langmuir maximum adsorption capacity, and b, kPa^{-1} – Langmuir equation constant, q is the adsorption capacity at pressure p, cm^3/g STP, k is the constant defining the adsorption capacity at a pressure of 1 kPa, $cm^3/(g \cdot kPa^n)$, and n is the heterogeneity coefficient, −, $0 \leq n \leq 1$. Standard Temperature and Pressure (STP) conditions referred to a temperature of 25°C and pressure of 100 kPa.

Textural analysis included the characterisation of the pore space of the coals. Based on low-pressure isotherms, textural parameters were determined, in particular specific surface area, pore volume, and average pore size. Pore size distributions of individual coal samples were determined using density functional theory (DFT). In the calculations, the CO_2-DFT model was applied, assuming slit-shaped pores with sizes ranging from 0.4 to 1.1 nm (micropore range). Additionally, based on the Horvath-Kawazoe (H-K) theory with slit pore geometry, the volume and average size of micropores in the studied coals were determined. The micropore region was also analysed using Dubinin-Radushkevich (D-R) theory, describing the amount of CO_2 adsorbed in micropores.

2.3.2. Gravimetric adsorption method

CO_2 adsorption measurements were conducted under elevated pressure conditions at a temperature of 30°C. Gravimetric analyser IGA-001 (Hiden Isochema, United Kingdom) was used to obtain adsorption isotherms on coal samples with a grain fraction of 0.16 ÷ 0.25 mm. Prior to the measurements, dry coals weighing approximately 0.4 g were degassed at 80°C under high vacuum (~10^{-6} kPa) for 720 min. The adsorption capacity was measured for several CO_2 equilibrium pressures, 100, 500 and 1200 kPa, respectively. The obtained adsorption data were approximated using Langmuir, Freundlich, and Langmuir-Freundlich (LF) models of the isotherm in order to determine the fitted quantity adsorbed of CO_2.

2.3.3. CO_2 adsorption kinetics study

The diffusion rate of CO_2 in the coal pores was analysed based on changes in the mass of the coal sample over time, recorded during gravimetric measurements. The analysis was carried out for isothermal and isobaric conditions of the adsorption process, within a linear segment of the isotherm (saturation from vacuum up to 100 kPa). Using a unipore model, based on Fick's second law, the effective diffusion coefficient D_e was determined. The value of the effective

diffusion coefficient was calculated using Timofeev's formula for the time $t_{1/2}$, at which the amount of adsorbed gas equals half of the final amount [29]:

$$D_e = \frac{0.308 r^2}{\pi^2 t_{1/2}} \tag{3}$$

where: $t_{1/2}$ – adsorption half-time, s; r – equivalent radius calculated from the formula: $r = \frac{1}{2}\sqrt[3]{\frac{2 \cdot d_1^2 \cdot d_2^2}{d_1 + d_2}}$ [cm]; d_1, d_2 – lower and upper diameter in the tested grain fraction.

The diffusion kinetics were analysed in relation to the degree of coalification and the texture of the examined Upper Silesian coals.

3. Results

3.1. Characteristics of the coal samples

TABLE 1 presents the designations and main characteristics of the studied hard coal samples. Coals varied in ash (from 2.69 to 7.54%) and moisture (from 0.53 to 1.59%) contents with average density of 1.392 g/cm^3.

TABLE 1

Results of technical and microscopic analysis

Coal sample	Member/ beds	R_0 [%]	Coal rank	Vt [%]	In [%]	Lt [%]	V^{daf} [%]	ρ_{He} [g/cm^3]	A^d [%]	W_t [%]
AZ	Poruba	0.85	Medium Ortho C bituminous	88.03	8.85	3.12	40.16	1.399	7.22	0.83
ZF1	Załęże	1.06	Medium Meta B bituminous	60.44	36.34	3.24	20.92	1.326	2.69	1.59
ZF2	Ruda	1.07	Medium Meta B bituminous	87.55	9.78	2.67	20.20	1.324	5.56	0.88
CR1	Hrušov	1.65	Medium Per A bituminous	79.04	20.96	0	15.49	1.513	5.58	0.53
CR2	Hrušov	1.94	Medium Per A bituminous	91.29	8.71	0	13.62	1.403	7.54	0.62
CR3	Hrušov	2.03	High Para C anthracite	78.60	21.40	0	12.80	1.387	6.87	0.55

ρ_{He}: helium density, V^{daf}: volatile matter with dry-ash-free basis, A^d: ash content with dry basis, W_t: moisture content with air-dried basis, R_0: mean vitrinite reflectance, Vt: vitrinite, In: inertinite, Lt: liptinite.

In this study, coal rank resulting from the degree of coalification of the coal matrix was expressed by the vitrinite reflectance coefficient (R_0). According to the literature, a higher degree of coalification corresponds to a higher content of the C element in the coal matrix [21]. As it may be seen from TABLE 1, the mean vitrinite reflectance of the analysed coal samples covered a range of R_0 values from 0.85% to 2.03%, with volatile matter content ranging from 12.80% to 40.16%. According to the UN-ECE classification, these were primarily medium-rank bituminous coals (from A to C), as well as high-rank anthracite coal [30]. As shown in Fig. 2a,

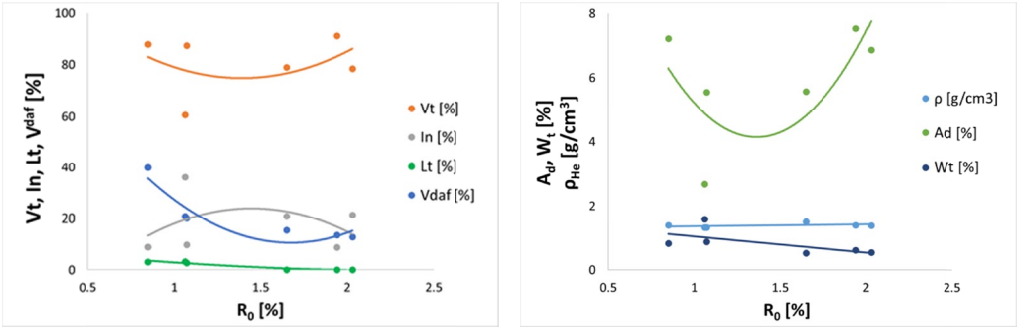

(a) (b)

Fig. 2. Trends in parameter variability with the coalification degree of the coal samples: (a) the content of main maceral groups and volatile matter, (b) helium density, moisture and ash contents

the studied coals differed in maceral composition, which was partly a result of variations in the coalification degree [31].

A nonlinear decreasing relationship was observed between vitrinite reflectance (R_0), which defines coal rank, and volatile content (V^{daf}). An increasing degree of coalification was accompanied by a reduction in volatile matter content of coal. The vitrinite content varied, with the coals exhibiting a U-shaped trend, showing a minimum of vitrinite content and a maximum of inertinite content at R_0 around 1.5%. As shown in Fig. 2b, coals with $R_0 > 1.5\%$ exhibited a disappearance of liptinite group macerals. With a higher R_0, a decrease in total moisture was observed. Ash content ranged from 2.69% to 7.54%. Within the analysed range of R_0, helium density exhibited a similar variability trend to that observed for vitrinite macerals group.

3.2. Texture of different rank coals

Fig. 3 presents the low-pressure CO_2 adsorption isotherms determined at 0°C for the studied coals of different rank. Within the measured pressure range of 0-100 kPa, the best approximation

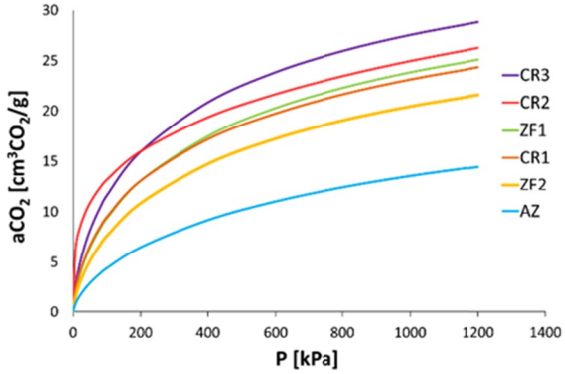

Fig. 3. Low-pressure CO_2 adsorption isotherms at 0°C for the studied coals

of experimental data was achieved using the Langmuir model (see determination coefficients in TABLE 2). The Freundlich model resulted in slightly lower quality of approximation for the low-pressure isotherm.

According to the isotherms presented in Fig. 3, the highest adsorption capacity was exhibited for the sample with the highest coalification degree – high-rank Para C anthracite coal CR3 (18.614 cm^3/g), followed by medium-rank Per A bituminous coal CR2 (18.072 cm^3/g). The lowest adsorption capacity was observed in the low rank coal sample – medium-rank Ortho C bituminous AZ (9.801 cm^3/g). It is noteworthy that the CO_2 adsorption capacity of AZ coal was more than half that of the highest-rank coals CR2 and CR3. Coal ZF2, classified as a medium-rank Meta B bituminous, also showed poor adsorption properties with a CO_2 adsorption capacity of 11.433 cm^3/g. The medium-rank, Meta B (ZF1) and Per A (CR1) bituminous coals exhibited very similar properties, with the quantity adsorbed of CO_2 around 14 cm^3/g.

TABLE 2

Carbon Dioxide at 0°C: fitting parameters of Freundlich and Langmuir models

Sample	AZ	ZF1	ZF2	CR1	CR2	CR3
Freundlich model						
n	0.485	1.077	0.667	1.119	1.033	1.291
k	0.660	0.570	0.627	0.558	0.631	0.574
R^2	0.9941	0.9947	0.9932	0.9935	0.9943	0.9908
Langmuir model						
a_m, cm^3/g STP	15.540	20.277	17.507	20.747	22.234	23.950
b, 1/kPa	0.0164	0.0232	0.0186	0.0210	0.0212	0.0254
R^2	0.9999	0.9973	0.9990	0.9977	0.9989	0.9989
Adsorption capacity						
$q\,CO_2$, cm^3/g STP	9.801	14.092	11.433	13.868	18.072	18.614

$q\,CO_2$, cm^3/g STP – adsorption capacity of coal at a pressure of 100 kPa (model value).

TABLE 3 presents a summary of the textural parameters of the studied coals obtained from the analysis of low-pressure adsorption isotherms of CO_2 at 0°C. CO_2 adsorption within the pressure range up to 100 kPa limits the analysis to pores narrower than 1.1 nm, thus enabling the characterisation of the ultra-microporous structure of coals.

Analysing the textural parameters from TABLE 3, it can be observed that the Langmuir surface area ranged from 63.2 to 109.4 m^2/g depending on the coal sample. Samples with the highest coal rank exhibited significantly higher surface areas compared to the other samples. They also had the largest pore volumes, amounting to 0.0281 cm^3/g for coal CR2 and 0.0323 cm^3/g for coal CR3. The Langmuir surface areas for ZF1 and CR1 were, on average, 14-16% lower than in the highest-rank coals. The pore volumes of these samples were slightly smaller than those of CR2 and CR3, measuring approximately 0.026 cm^3/g. The coal samples with the lowest degree of coalification showed a Langmuir surface area of 79.9 m^2/g for coal ZF2 and 63.2 m^2/g for coal AZ. The lowest surface area corresponded to the lowest measured pore volumes, which were 0.0177 cm^3/g for coal AZ and 0.0212 cm^3/g for coal ZF2.

Specific surface area determined according to the BET theory was also analysed. This is particularly important when characterising ultra-microporous materials. Hard coals belong to specific materials, for which adsorption measurements at a low temperature (usually −196°C)

TABLE 3

Carbon Dioxide at 0°C: Textural properties of the studied coals

Sample	AZ	ZF1	ZF2	CR1	CR2	CR3
Surface area, pore size						
S_{BET}, m^2/g	57.79	93.29	74.86	89.05	103.65	103.99
S_{LA}, m^2/g	63.2	92.6	79.9	94.8	101.6	109.4
d_{LA}, nm	0.47	1.60	1.13	1.65	1.08	1.18
Horvath-Kawazoe						
V_{PH-K}, cm^3/g)	0.0177	0.0265	0.0212	0.0260	0.0281	0.0323
d_{H-K} (nm)	0.43	0.39	0.40	0.39	0.39	0.39
DFT						
V_{DFT}, cm^3/g	0.0061	0.0238	0.0249	0.0257	0.0226	0.0262
Dubinin-Radushkevich						
MC_{DR}, cm^3/g STP	18.095	31.638	25.970	33.018	31.427	36.277
MV_{DR}, cm^3/g STP	0.0321	0.0579	0.04754	0.0564	0.0575	0.0664

S_{BET} (m^2/g) – multipoint surface area according to BET; S_{LA} (m^2/g) – Langmuir surface area; d_{LA}, nm – average pore diameter based on the 4V/A by Langmuir; V_{PH-K} (cm^3/g) – maximum pore volume according to the Horvath-Kawazoe slit pore model at p/p° = 0.029; d_{H-K} (nm) – average pore width based on the Horvath-Kawazoe slit pore geometry; V_{DFT} (cm^3/g) -micropore volume according to the DFT model; MC_{DR}, cm^3/g STP – Dubinin-Radushkevich micropore capacity; MV_{DR}, cm^3/g STP – Dubinin-Radushkevich micropore volume.

are incomparable. Under such conditions, the pore structure of coal is not fully accessible to adsorbed molecules (usually N_2) due to the adsorption requiring a certain activation energy [32]. Adsorption measurement with CO_2 at 0°C is useful for analysing materials with narrow micropores. At this temperature, diffusion becomes faster compared to lower temperatures, e.g. liquid nitrogen temperature. As shown in TABLE 3, the BET specific surface area was similar to that obtained using the Langmuir model. It is worth noting that the average pore diameter was about 1.1 nm for the coals with the highest degree of coalification (samples CR2, CR3 and ZF2). For coals with an intermediate degree of coalification (ZF1 and CR1), the average pore diameter was larger, about 1.6 nm, whereas the smallest average pore size, amounting to 0.47 nm, was found for AZ coal with the lowest degree of coalification.

Micropore capacity and micropore volumes obtained by the D-R method showed slightly higher maximum adsorption values compared to those from the Langmuir model (see TABLE 2), as well as increased micropore volumes compared to the DFT and Horvath-Kawazoe methods (see TABLE 3). According to some authors, based on CO_2 gas adsorption at 0°C on coals, the Dubinin-Radushkevich theory analyses experimental data better than monolayer or multilayer models [33].

Fig. 4(a)-(c) presents incremental pore size distributions obtained using density functional theory (DFT), applying the CO_2-DFT model on coal and assuming a slit-pore model. The presented plots make it possible to assess the effect of the degree of coalification on the pore structure of coal. According to Fig. 4, the studied coals exhibited multimodal micropore distributions, which undergo certain qualitative changes resulting from the complex process of coalification of the coal substance [31]. The main peaks visible in the distributions are concentrated around 0.5-0.7 nm and 0.8-0.9 nm. Two medium-rank coal samples, CR1 and ZF2, additionally showed a pronounced peak in the microporous region with pore diameters of about 1.0 nm. All the coal samples contained

pores with diameters <0.7 nm (ultramicropores), which play a particularly important role in gas adsorption on coal. From Fig. 4(d), which presents cumulative pore volume, it follows that the volume of ultramicropores (d < 0.7 nm) increased with the degree of coalification. If we look at the final values of the plots from Fig. 4(d), it can be seen that all samples had a similar micropore volume, ranging from 0.023 to 0.026 cm^3/g. The highest micropore volume was found for the highly carbonized CR3 and CR1 samples, whereas the lowest microporosity of 0.006 cm^3/g was observed for the weakly carbonized sample AZ (see Fig. 3(b)). It is worth emphasising that in samples CR1 and ZF2 a significant increase in the volume of micropores with sizes ~1.0 nm was recorded at the point where the peaks appear on the incremental plot (see Fig. 4(b)).

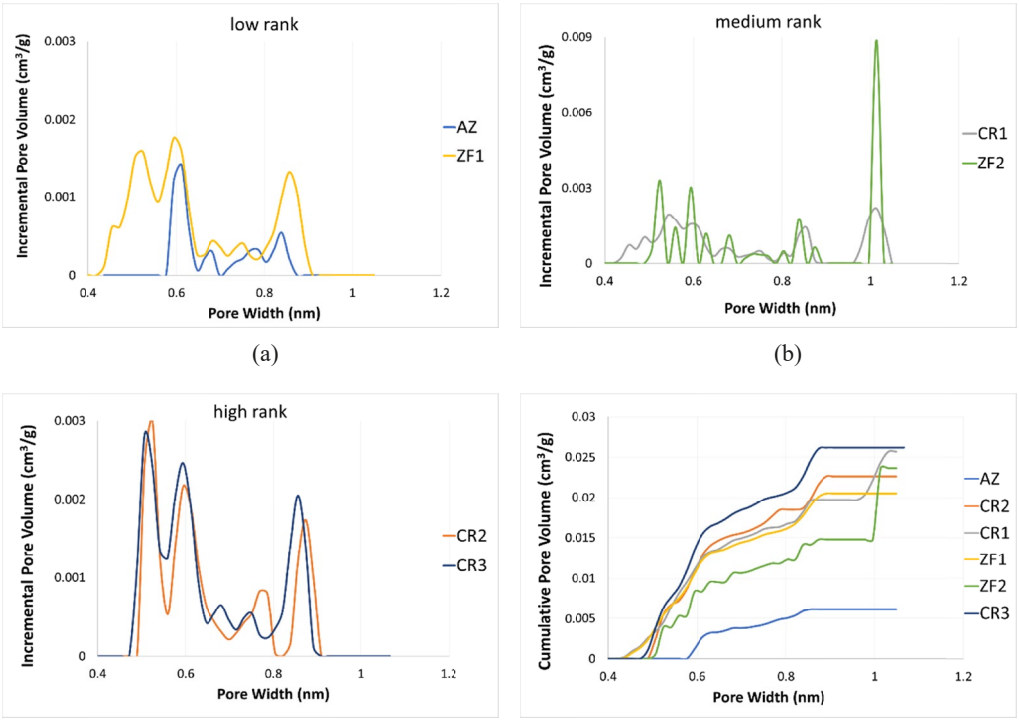

Fig. 4. Pore size distribution calculated by Density Functional Theory to the CO_2 adsorption isotherm at 0°C: incremental pore volume vs. pore width for coals with (a) low, (b) medium and (c) high degree of coalification; (d) cumulative pore volume vs. pore width

The analysis of the results obtained using the Horvath-Kawazoe method (see TABLE 3) showed that the micropore volume increased in the studied coals in line with the trend of increasing degree of coalification. The average micropore width, on the other hand, remained practically unchanged, being 0.40 nm in lower rank coals with $R_0 \leq 1$, and slightly smaller, 0.39 nm, in coals with $R_0 > 1$. This observation confirmed the assumption of the existence of an ultra-micropore region in all the studied coals, regardless of coal rank.

3.3. CO_2 adsorption at near-seam temperature

3.3.1. Isotherm analysis

The experimental amounts of CO_2 adsorbed at 30°C under elevated pressures were approximated using two isotherm models, Langmuir and Freundlich (see Fig. 5). As a result of both models fitting to determine the fitted quantity adsorbed, it was established that the Freundlich equation better describes CO_2 adsorption on coals (see TABLE 4).

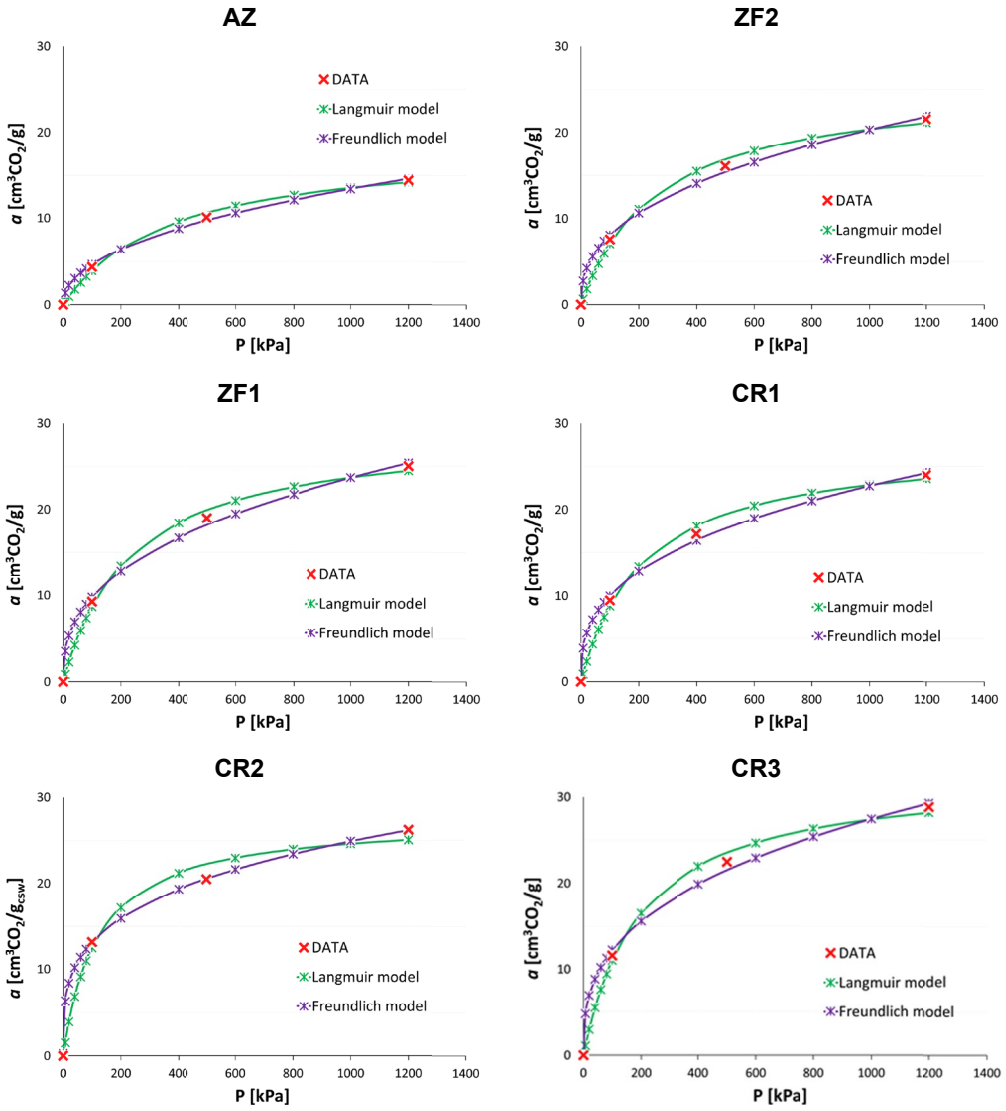

Fig. 5. CO_2 adsorption isotherms at 30°C with fitted Freundlich and Langmuir models

TABLE 4

Fitting parameters for Freundlich, Langmuir and Langmuir-Freundlich (LF) isotherm models

Sample	AZ	ZF1	ZF2	CR1	CR2	CR3
Freundlich						
n	0.459	0.382	0.401	0.356	0.277	0.352
k	0.565	1.696	1.277	1.946	3.679	2.420
R^2	0.9951	0.997	0.997	0.9971	1.00	0.997
Langmuir						
a_m	18.676	29.399	25.815	27.827	27.610	32.846
b	0.003	0.004	0.004	0.0046	0.008	0.005
R^2	0.990	0.9971	0.9970	0.9955	0.945	0.9969
LF						
b	0.00073	0.001440	0.001358	0.001726	0.0022381	0.001934
n	0.678	0.656	0.677	0.646	0.522	0.651
a_m	30.292	42.592	37.042	39.007	41.202	45.489
R^2	1.00	1.00	1.00	1.00	0.998	1.00

R^2 – dimensionless coefficient of determination.

Due to the limitations of both models, manifested as underestimation of the adsorbed amount in individual CO_2 pressure ranges, a model suitable for heterogeneous adsorption systems had previously been developed. The Langmuir-Freundlich (LF) isotherm model results from a combination of the Langmuir and the Freundlich equations [34]. The LF model describes the amount of CO_2 adsorbed on coal with the following equation:

$$\frac{a}{a_m} = \frac{(bp)^n}{1+(bp)^n} \tag{4}$$

The LF model makes it possible to estimate the CO_2 contents not taken into account by the Langmuir model at the low equilibrium pressures (0-100 kPa). Subsequently, the LF model corrects the shortcomings of the Freundlich model, i.e. by estimating the not included CO_2 contents in the range 200-1000 kPa and eliminating the excess amounts imposed by the increasing adsorbate concentration (>1000 kPa). This approach optimises the course of the CO_2 isotherm on hard coal over a wide range of coalification degree. Additionally, the LF model predicts monolayer adsorption at higher CO_2 pressures in accordance with the Langmuir isotherm. The Langmuir-Freundlich equation (1) for $n = 1$ reduces to the Langmuir equation.

Fig. 6 presents the optimisation of the adsorption model fitting to the experimental data, taking as an example coal CR3. As can be seen from TABLE 4, the application of the LF equation resulted in a significant improvement in the quality of the experimental data description. Only after applying the combined Langmuir and Freundlich equations (LF model) was an adequate fitting quality achieved. Consequently, Fig. 7 compiles all the isotherm curves of the optimal fit to the experimental points. Only in the case of one coal did the Freundlich model yield a better fit than the combined LF equation model (see TABLE 4, sample CR2). For none of the coals was the value of the parameter n equal to unity.

The highest adsorption capacity for CO_2 was exhibited by the highly coalified coal CR3, and the lowest by the coal AZ of the low coalification degree. The obtained results corresponded to the specific surface areas of the individual samples and the micropore volumes (see TABLE 3).

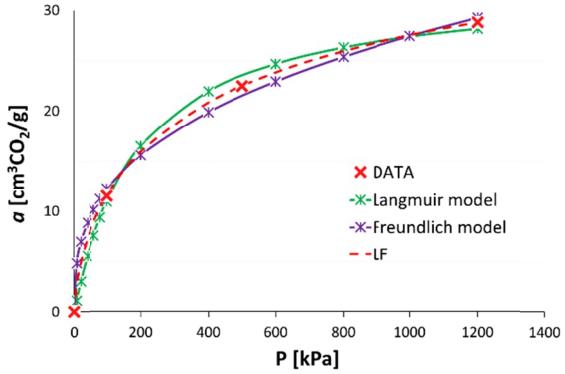

Fig. 6. Optimisation of the adsorption model fit to the experimental data on the example of coal CR3

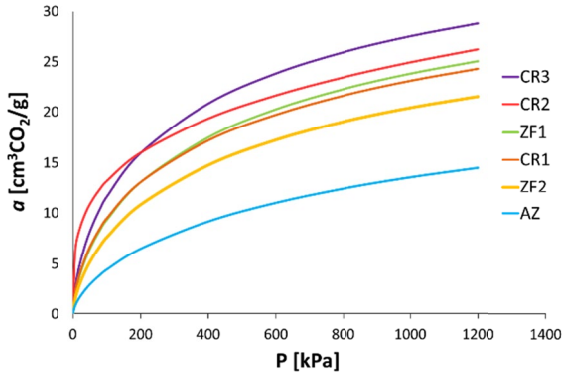

Fig. 7. Compilation of CO_2 adsorption isotherms at 30°C for the studied coals

3.3.2. Kinetics of CO_2 adsorption

Fig. 8(a) presents a comparison of CO_2 adsorption kinetics obtained for the respective equilibrium pressure levels. To analyse the rate of adsorption, both a quantitative comparison of the curves (Fig. 8(b)) and a qualitative one (normalised curves, Figs. 8(c) and 8(d)) were carried out. As can be seen, the time required for CO_2 saturation varied depending on the degree of coalification. TABLE 5 summarises the values of the adsorption half-time ($t_{1/2}$) and of the effective diffusion coefficient (D_e) resulting from the transport properties of coal.

The CO_2 adsorption half-time ranged from 230.5 to 811.74 s. The highest adsorption rate was observed for the coal sample with the highest coal rank, CR3, while adsorption was the slowest in the case of coal CR1, which had an intermediate coal rank among the studied samples. Medium-rank coals with R_0 from 0.848 to 1.071% had similar half-times. The values of the effective diffusion coefficient, based on the given CO_2 adsorption half-times, ranged from $4.05 \cdot 10^{-9}$ cm^2/s to $13.31 \cdot 10^{-9}$ cm^2/s. The fastest CO_2-adsorbing samples, i.e. coals CR2 and CR3, had the most homogeneous pore structure, comprising voids with three dominant pore sizes: 0.5, 0.6 and 0.85 nm (see Fig. 4(c)). In the case of sample CR1, in which CO_2 diffusion through the porous

TABLE 5

Kinetic properties in relation to CO_2

Sample	$a_{1/2}$	$t_{1/2(CO_2)}$ [s]	$D_{e(CO_2)} \cdot 10^{-09}$ [cm^2/s]
AZ	2.2151	758.22	4.05
ZF1	4.5816	727.20	4.22
ZF2	3.8368	767.10	4.00
CR1	4.7840	811.74	3.78
CR2	6.5898	604.56	5.08
CR3	6.5485	230.5	13.31

structure was the slowest, the pore size distribution was the most heterogeneous. The predominant part of the microporous structure of this coal comprised various pore sizes in the range from 0.4 to 0.8 nm. Only two dominant peaks at 0.85 nm and around 1.0 nm indicated some ordering of the pore structure; however, their contribution to the overall coal porosity was only ca. 20%.

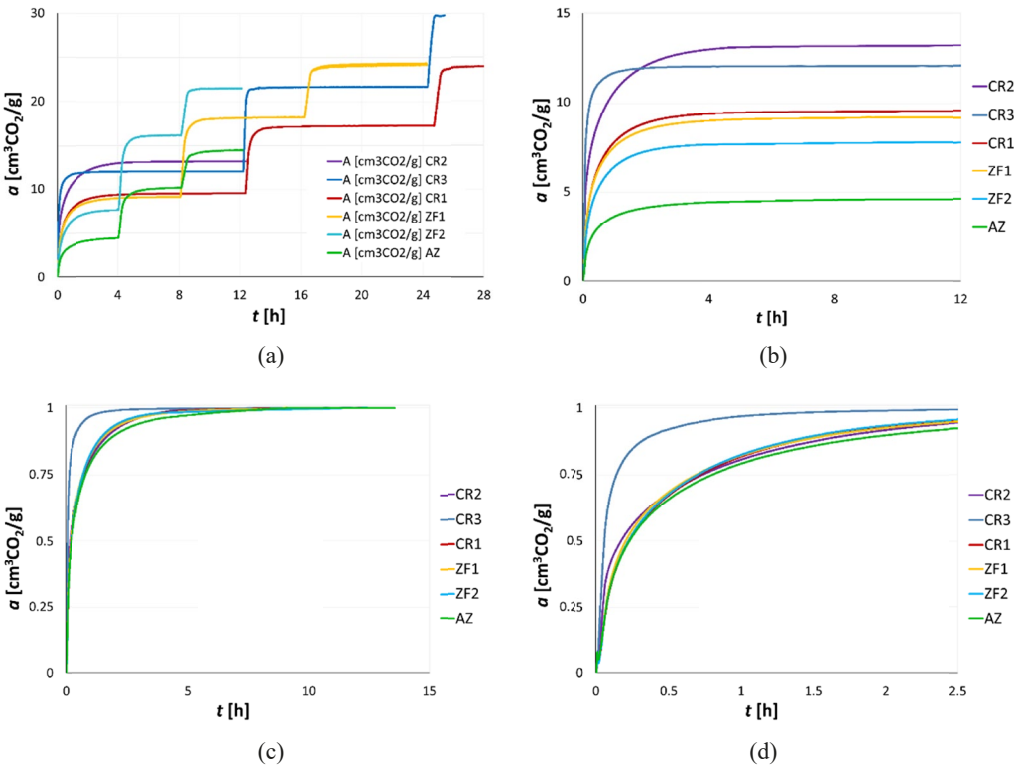

Fig. 8. Comparison of CO_2 adsorption kinetics at 30°C

The study showed that the pore structure of coal is crucial in the analysis of the adsorption performance of coals. It determines the value of the effective diffusion coefficient, which

reflects the transport properties of coal. The diffusion rate was not hindered by a high degree of coalification but rather by structural heterogeneity of pores, which can be detected by examining the pore size distribution. No correlation was found between the content of the main maceral groups and CO_2 adsorption capacity or the kinetics of CO_2 adsorption. These issues will require separate studies.

4. Summary and conclusions

The studies carried out confirmed differences in pore structure and CO_2 adsorption properties of different rank coals. It has been shown that the specific surface area and micropore volume of coal samples developed due to the increasing coalification. The development of coal porosity with increasing coalification was confirmed. All the coal samples demonstrated narrow micropores with sizes <0.7 nm, referred to as ultramicropores. It was shown that micro- and ultramicropores have the dominant contribution to the specific surface area of coals. CO_2 adsorption isotherm modelling showed that no single model might work as a universal and adequately describe adsorption in both, at low-pressures as well as at elevated equilibrium pressures. Thus, the choice of the model of isotherm depended on the measured pressures. Implementation of the combined model (LF) was not always the optimal solution, although it proved suitable for most samples (5 out of 6). Analysis of pore size distributions by the DFT method, in the range up to 1.1 nm, revealed the main changes that occurred in the pore structure of the examined coals due to coalification degree. With the development of microporosity in higher-rank coals, an increase in the rate of CO_2 adsorption over time was observed, as indicated by the adsorption half-time $t_{1/2}$ and the effective CO_2 diffusion coefficient of coal. Studies based on the comprehensive characterisation of coal material and its adsorption properties remain relevant. The variability of coal properties is enormous, whereas adsorption methods help to differentiate samples from one another and provide qualitative information. Nevertheless, in the case of coal, analysis of pore space by adsorption methods remains a challenging task, primarily due to variations in surface accessibility at different temperatures and differences in the results obtained from a considerable number of adsorption models. As the results were obtained for dry samples, it should be noted that further tests on wet coals are required to fully assess the CCS/ECBM scenarios. In this study, it was established that coal pore structure is crucial in the analysis of the adsorption performance of coals and determines the transport properties of coal. The diffusion rate was not limited by the high rank of coal but rather by the structural heterogeneity of the pores, which could be detected by the analysis of the pore size distribution.

Acknowledgements

The research was funded in the framework of the statutory works of the Strata Mechanics Research Institute of the Polish Academy of Sciences.

References

[1] B. Dutka, Influence of Depth on CO_2/CH_4 Sorption Ratio in Deep Coal Seams. Sustainability **16**, 1, 43 (2023). DOI: http://dog.org/10.3390/su16010043

[2] M. Safaei-Farouji, D. Misch, R.F. Sachsenhofer, A review of influencing factors and study methods of carbon capture and storage (CCS) potential in coals. Int. J. Coal Geol. **277**, 104351 (2023). DOI: http://dog.org/10.1016/j.coal.2023.104351

[3] X. Du et al., CO_2 and CH_4 adsorption on different rank coals: A thermodynamics study of surface potential, Gibbs free energy change and entropy loss. Fuel **283**, 118886 (2021). DOI: http://dog.org/10.1016/j.fuel.2020.118886

[4] M. Chen, S. Masum, S. Sadasivam, H. Thomas, Modelling anisotropic adsorption-induced coal swelling and stress-dependent anisotropic permeability. International Journal of Rock Mechanics and Mining Sciences **153**, 105107 (2022). DOI: http://dog.org/10.1016/j.ijrmms.2022.105107

[5] H.H. Lee, H.J. Kim, Y. Shi, D. Keffer, C.H. Lee, Competitive adsorption of CO_2/CH_4 mixture on dry and wet coal from subcritical to supercritical conditions. Chemical Engineering Journal **230**, 93-101 (2013). DOI: http://dog.org/10.1016/j.cej.2013.06.036

[6] H.J. Kim, Y. Shi, J. He, H.H. Lee, C.H. Lee, Adsorption characteristics of CO_2 and CH_4 on dry and wet coal from subcritical to supercritical conditions. Chemical Engineering Journal **171**, 1, 45-53 (2011). DOI: http://dog.org/10.1016/j.cej.2011.03.035

[7] D. Bose et al., Innovative approaches for carbon capture and storage as crucial measures for emission reduction within industrial sectors. Carbon Capture Science & Technology **12**, 100238 (2024). DOI: http://dog.org/10.1016/j.ccst.2024.100238

[8] [ARCHIVED CONTENT] COP26 Goals – UN Climate Change Conference (COP26) at the SEC – Glasgow 2021. Accessed: Dec. 12, (2025). [Online]. Available: https://webarchive.nationalarchives.gov.uk/ukgwa/20230311034236/https://ukcop26.org/cop26-goals/

[9] T. Vangkilde-Pedersen et al., Assessing European capacity for geological storage of carbon dioxide – the EU GeoCapacity project. Energy Procedia **1**, 1, 2663-2670 (2009). DOI: http://dog.org/10.1016/j.egypro.2009.02.034

[10] S.A. Masum, M. Chen, L.J. Hosking, K. Stańczyk, K. Kapusta, H.R. Thomas, A numerical modelling study to support design of an in-situ CO_2 injection test facility using horizontal injection well in a shallow-depth coal seam. International Journal of Greenhouse Gas Control **119**, 103725 (2022). DOI: http://dog.org/10.1016/j.ijggc.2022.103725

[11] B. Dutka, K. Godyń, Predicting variability of methane pressure with depth of coal seam. Przemysl Chemiczny **97**, 8, 1344-1348 (2018). DOI: http://dog.org/10.15199/62.2018.8.20

[12] M. Mastalerz, L. He, Y.B. Melnichenko, J.A. Rupp, Porosity of Coal and Shale: Insights from Gas Adsorption and SANS/USANS Techniques. Energy and Fuels **26**, 8, 5109-5120 (2012). DOI: http://dog.org/10.1021/ef300735t

[13] H. Li et al., A Comparative Investigation of the Adsorption Characteristics of CO_2, O_2 and N_2 in Different Ranks of Coal. Sustainability **15**, 10, 8075 (2023). DOI: http://dog.org/10.3390/su15108075

[14] T.N. Tambaria, Y. Sugai, F. Anggara, Experimental measurements of CO_2 adsorption on Indonesian low-rank coals under various conditions. J. Pet. Explor. Prod. Technol. **13**, 3, 813-826 (2023). DOI: http://dog.org/10.1007/s13202-022-01569-z

[15] K. Dong, Z. Zhai, A. Guo, Effects of Pore Parameters and Functional Groups in Coal on CO_2/CH_4 Adsorption. *ACS* Omega **6**, 48, 32395-32407 (2021). DOI: http://dog.org/10.1021/acsomega.1c02573

[16] S. Sadasivam, S. Masum, M. Chen, K. Stańczyk, H. Thomas, Kinetics of Gas Phase CO_2 Adsorption on Bituminous Coal from a Shallow Coal Seam. Energy & Fuels **36**, 15, 8360-8370 (2022). DOI: http://dog.org/10.1021/acs.energyfuels.2c01426

[17] S.A. Masum, S. Sadasivam, M. Chen, H.R. Thomas, Low Subcritical CO_2 Adsorption-Desorption Behavior of Intact Bituminous Coal Cores Extracted from a Shallow Coal Seam. Langmuir **39**, 4, 1548-1561 (2023). DOI: http://dog.org/10.1021/acs.langmuir.2c02971

[18] M. Li, Y. Long, L. Guo, S. Zeng, J. Li, L. Zhang, An Experimental Study on CO_2 Displacing CH_4 Effects of Different Rank Coals. Geofluids **1**, 6822908 (2022). DOI: http://dog.org/10.1155/2022/6822908

[19] S. Zheng et al., Measurement of CO_2 adsorption capacity with respect to different pressure and temperature in sub-bituminous: implication for CO_2 geological sequestration. Front Earth Sci. **17**, 3, 752-759 (2023). DOI: http://dog.org/10.1007/s11707-022-1026-x/metrics

[20] L. He, Y. . Melnichenko, M. Mastalerz, R. Sakurovs, A.P. Radlinski, T. Blach, Pore Accessibility by Methane and Carbon Dioxide in Coal as Determined by Neutron Scattering. Energy and Fuels **26**, 3, 1975-1983 (2012). DOI: http://dog.org/10.1021/ef201704t

[21] K. Godyń, B. Dutka, Sorption and Micro-Scale Strength Properties of Coals Susceptible to Outburst Caused by Changes in Degree of Coalification. Materials **14**, 19, 5807 (2021). DOI: http://dog.org/10.3390/ma14195807

[22] L.L. Liu et al., Pore Size Distribution Characteristics of High Rank Coal with Various Grain Sizes. *ACS* Omega **5**, 31, 19785-19795 (2020). DOI: http://dog.org/10.1021/acsomega.0c02569

[23] E.S. Bickford et al., On the adsorption affinity coefficient of carbon dioxide in microporous carbons. Carbon N Y **42**, 8-9, 1867-1871 (2004). DOI: http://dog.org/10.1016/j.carbon.2004.02.026

[24] M. Skiba, B. Dutka, M. Młynarczuk, MLP-Based Model for Estimation of Methane Seam Pressure. Energies (Basel) **14**, 22, 7661 (2021). DOI: http://dog.org/10.3390/en14227661

[25] M.S. Masoudian, D. . Airey, A. El-Zein, Experimental investigations on the effect of CO_2 on mechanics of coal. Int. J. Coal Geol. **128-129**, 12-23 (2014). DOI: http://dog.org/10.1016/j.coal.2014.04.001

[26] C.M. White et al., Sequestration of carbon dioxide in coal with enhanced coalbed methane recovery – A review. Energy and Fuels **19**, 3, 659-724 (2005). DOI: http://dog.org/10.1021/ef040047w

[27] M. Sivek, J. Jirásek, L. Hýlová, Z. Mirkowski, Zawartość części lotnych w węglach kamiennych: parametr nie tylko chemiczno-technologiczny. Przegląd Geologiczny **66**, 8, 477-480 (2018). Accessed: Dec. 12, 2025. [Online]. Available: https://www.kurzy.cz

[28] Z. Klika, J. Serenčíšová, A. Kožušníková, I. Kolomazník, S. Študentová, J. Vontorová, Multivariate statistical assessment of coal properties. Fuel Processing Technology **128**, 119-127 (2014). DOI: http://dog.org/10.1016/j.fuproc.2014.06.029

[29] D.P. Timofeev, The mechanism of transport of matter in porous sorbents. Russian Chemical Reviews **29**, 3, 180-192, (1960). DOI: http://dog.org/ 10.1070/rc1960v029n03abeh001226

[30] UN. ECE. C. on S. Energy, UN. ECE. C. on Energy. W. P. on Coal, and UN. ECE. G. of E. on the U. and P. of S. Fuels, International Classification of in-Seam Coals =: Classification internationale des charbons en veine = Mezhdunarodnaia klassifikatsiia uglei v plastakh. 1998, UN,. Accessed: Dec. 12, 2025. [Online]. Available: https://digitallibrary.un.org/record/260911

[31] D.A. Wood, Complex interactions between coal maceral fractions, thermal maturity, reaction kinetics, fractal dimensions and pore-size distributions: Implications for gas storage. Int. J. Coal Geol. **305**, 104788 (2025). DOI: http://dog.org/10.1016/j.coal.2025.104788

[32] O. P. Mahajan, CO_2 surface area of coals: The 25-year paradox. Carbon N Y **29**, 6, 735-742 (1991). DOI: http://dog.org/10.1016/0008-6223(91)90010-g

[33] Z. Liu, Z. Zhang, S.K. Choi, Y. Lu, Surface Properties and Pore Structure of Anthracite, Bituminous Coal and Lignite. Energies **11**, 6, 1502 (2018). DOI: http://dog.org/10.3390/en11061502

[34] J. Serafin, B. Dziejarski, Application of isotherms models and error functions in activated carbon CO2 sorption processes. Microporous and Mesoporous Materials **354**, 112513 (2023). DOI: http://dog.org/10.1016/j.micromeso.2023.112513